

# **Ground S-band hybrid AESA antenna, moving from concept to measurement results of the prototype**

A. Lohou, B. Lesur, G. Kipfer  
SAFRAN DATA SYSTEMS  
La Teste de Buch, France

P.-M. Bastie  
SAFRAN DATA SYSTEMS Inc  
Norcross, GA 30071, USA  
pm.bastie@safrandatasystems.com

## **ABSTRACT**

The contribution talks about the application of AESA technology for telemetry ground antennas. The AESA concept we are proposing is a 1-axis electronically steerable antenna (elevation axis), while the azimuth axis remains mechanically driven. The design will lead to a 1m<sup>2</sup> antenna, dedicated to short - medium range telemetry, with potential high target dynamics. This paper introduces the concept and details the design with the first mock-up, which was manufactured and measured. The results present a very important knowledge in the establishment of phase controls for beam-steering, and in the control of the axial ratio. Then, this document focuses on the development of a complete prototype for an evaluation at the end of 2022.

## **INTRODUCTION**

Nowadays, needs for ground telemetry are covered by reflector antennas for high gain applications, or by small passive panels for smaller gain applications. Safran Data Systems offers a wide variety of products ranging from small-size panel to large reflector antennas (1.8 m to 9.3 m diameter) in L, S and C bands for these applications [1]. In order to complete its product range, and to propose innovative solutions, Safran Data Systems carries out an R&D effort on electronically steerable solutions for these applications. Indeed, these promising technologies would allow to offer new possibilities such as faster tracking and a low-gain mode for targets in a close perimeter. There is also a reduction of mechanics for the hybrid steering antenna and a complete removal of mechanics for the fully electronically steered antenna, with other functions, such as multi-beam capacity.

This publication fits into this context of development of a 1-D electronically steerable antenna in S-band. The scope of the article is limited to the implementation and experimental characterization of a 4x4 elements electronically steered antenna array which will allow to validate the working principle and performance on a smaller size and with remote active electronics, before embracing the next steps of development.

In the next part, the architecture of the antenna will be presented. Then, the design and modelling of the 4x4 array will be tackled, with an emphasis on the unit-cell of this array. Finally, experimental results will conclude the article.

## **ARCHITECTURE**

Test range telemetry applications require full hemispherical coverage with optimal performance at low elevation. The use of planar electronically steered antennas is then prohibited due to the

loss of performance at low elevation angles. The chosen solution consists of orientating the antenna towards the test zone. Consequently, only an azimuthal sector is reachable, then, the panel has to be put on a mechanical positioner allowing continuous azimuthal rotation. The antenna is then orientated at  $45^\circ$  from the horizon and placed on a rotating axis (Figure 1). The electronic steering over  $\pm 45^\circ$  in elevation, coupled to the  $360^\circ$  mechanical rotation will allow to cover the whole hemisphere while suffering reasonable loss at low elevation and zenith.

For this first hybrid steering product, specifications set by Safran Data Systems are the following:

- S-band: [2.2-2.4] GHz
- RHCP/LHCP simultaneously
- Gain: [26-28] dBic // G/T: [4.5-6] dB/K
- Elevation electronic steering:  $\pm 45^\circ$
- Az & El tracking ability

The required size of the antenna to meet the specifications is around  $1\text{m}^2$ . The 1 axis only electronic steering offers the possibility to loosen the inter-element spacing in the horizontal axis and leads to a rectangular array (form factor: 1:3) of  $16 \times 8$  elements. The manufacturing dimensional constraints do not allow to fabricate such an object in one piece, that is why, the panel is divided into 4 independent tiles of  $8 \times 4$  elements. This 4 quadrants division will also allow to implement the azimuth and elevation tracking functions [2].

The fact that the electronic steering is limited to one axis allows to simplify the design of the unit-cell and of beamforming networks. The phase shift can be implemented on the lines of the array, after each polarization of a line has been combined. The lines are then combined between them to form the radiation pattern of the complete array. The phase shifters can then be used for the beam steering and to dynamically minimize the axial ratio.

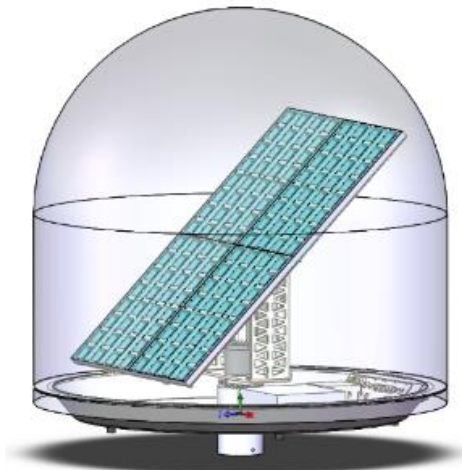


Figure 1 3-D view of the antenna orientated at  $45^\circ$  on its azimuthal positioner under its protection radome..

## DESIGN AND MODELLING OF THE $4 \times 4$ ARRAY

For this first  $4 \times 4$  elements prototype, we chose to use remote active circuits. This way, it is possible to partition the problem and to have increased freedom for the first tests. Therefore, the  $4 \times 4$  panel consists of the radiating cells and the combining networks of the horizontal lines. Each line is then connectorized, giving 8 connectors. The amplification, phase shifting and inter-line

combining are performed on a remote board using X-Microwave components (modular assembly of RF building blocks [3]).

Concerning the active circuits, a LNA (Gain: 22 dB; NF: 0.5 dB) and a phase shifter (4 bits; loss: 4 dB) were chosen because their performance match the G/T specification of our system. Note that the components used for the 4x4 mockup with the X-Microwave board are the same that will then be directly integrated on the back side of the final product.

The radiating element is a printed antenna placed into a cavity with an upper superstrate. The excitation is made by coupling stripline feeding lines through a slotted ground plane. This kind of unit-cell is used for its compactness and its performance in an array environment [4,5,6,7,8]. The use of a metallic cavity allows to widen the bandwidth and to mechanically hold the upper (superstrate) and lower (multilayer) PCBs..

As explained previously, electronically steering the beam in only one direction allows to widen the inter-element spacing along the orthogonal direction. Thus, the unit-cell is organized with a rectangular lattice (50% bigger on  $\lambda_{0,x}$  compared to  $\lambda_{0,y}$  @ 2.4 GHz), which allows to increase the surface while rejecting all grating lobes [9]. Key geometrical dimensions of the dual-polarization unit-cell were optimized to obtain an active reflection coefficient lower than -10 dB over [2.2-2.4] GHz up to 45° steering. The active reflection coefficients of both ports of the infinitely periodized unit-cell [10] can be seen on Figure 2.

Then, the simulation of the finite 4x4 panel made up of the radiating elements and the intra-lines Wilkinson combiners was performed. That simulation gives an 8 port (4 lines x 2 polarizations) [S]-matrix and 8 radiating patterns which will be used to synthesize the performance and the commands to be sent to the phase shifters.

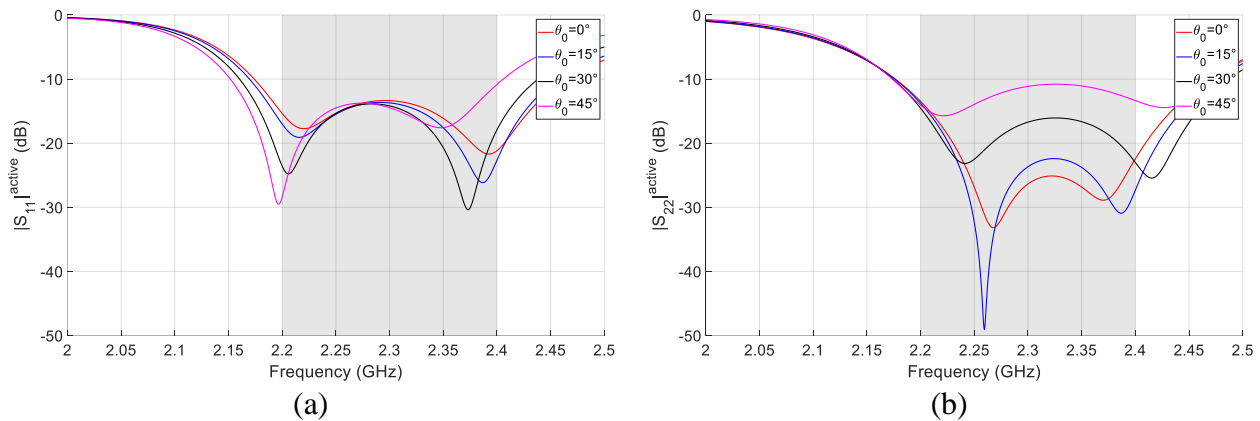


**Figure 2 Active matching of port 1 (a) and port 2 (b) of the infinitely periodized unit-cell.**

The front side of the multilayer PCB, with rooms for the 8 connectors, is shown on Figure 3, where is also shown the port numbering and the coordinate system used for experimental characterization. The simulated and measured reflection coefficients of the 8 ports of the panel are presented in Figure 4. We can see a good agreement between simulations and measurements; moreover, the matching is better than -10 dB over the whole bandwidth. Radiation pattern measurement of port 3 (center line, V-polarized) in both principal planes is shown in Figure 5 and Figure 6. A comparison with simulations allows to see a very good agreement between measurements and simulations on both polarizations and in both planes, whether on the main

lobe, nulls and side lobes. Only 1 port is presented here, but all the radiation patterns of the panel show the same agreement between simulation and measurement.

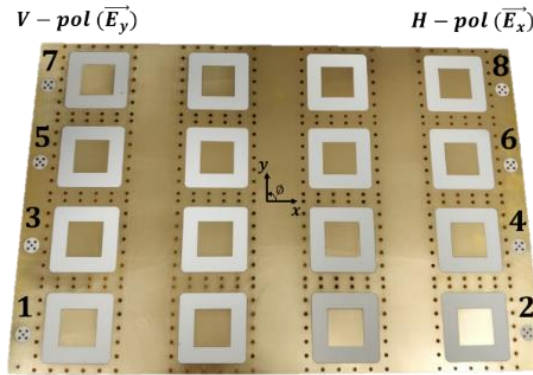


Figure 3 Multilayer PCB of the 4x4 panel.

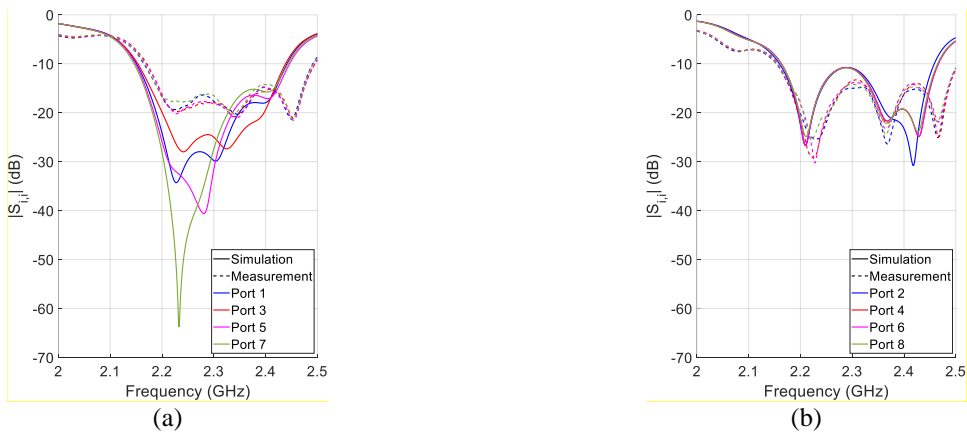


Figure 4 Reflection coefficients of V-polarization (a) and H-polarization (b) ports of the 4x4 panel.

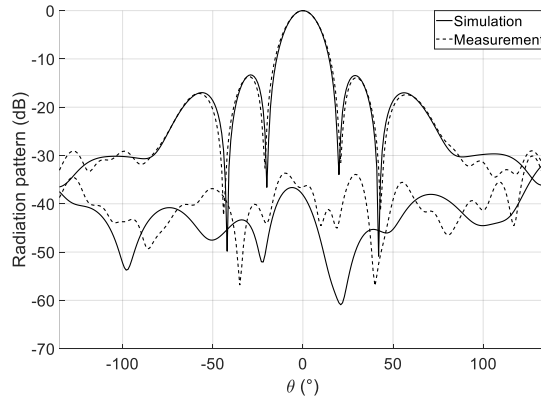
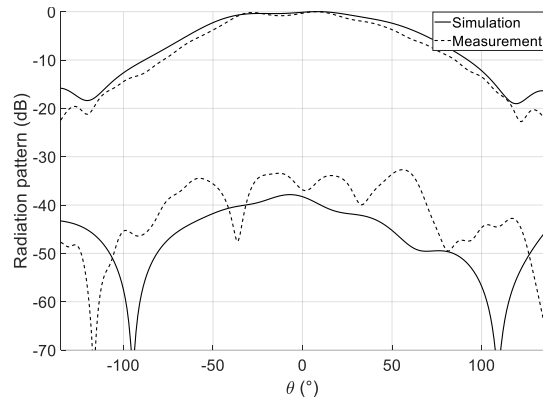


Figure 5 Radiation pattern of port 3 of the 4x4 panel at 2.25 GHz for  $\phi=0^\circ$ .



**Figure 6 Radiation pattern of port 3 of the 4x4 panel at 2.25 GHz for  $\phi=90^\circ$ .**

Once the 4x4 panel has been fully characterized, its 8 ports were connected to the 8 ports of the X-Microwave board containing the active circuits (LNAs and phase shifters) and combiners, through semi-rigid coaxial cables. One can see the panel and the X-microwave board mounted on their characterization stand in the anechoic chamber on Figure 7.

Independent measurements of the 4x4 panel and the active components were then coupled to the implementation of a driving and testing bench (Figure 8). On one hand, the computing part of the bench takes care of synthesising the commands to be sent to the phase shifters, function of the steering direction and taking into account the radiation patterns of the panel and the [S]-matrices of the panel and the various elements of the X-Microwave board. It is also possible to tune independently the phases of both polarizations in order to dynamically minimize the axial ratio if circular polarization operation is required. In that case, a hybrid coupler is used to combine H and V polarizations. On the other hand, the synthesized commands are transmitted to the phase shifters through an SPI bus driven by an Arduino board. Figure 9 shows the radiation patterns obtained for electronic steering from  $-45^\circ$  to  $+45^\circ$  in RHCP at 2.25 GHz. The patterns are well formed and the steering directions are respected. The cross-polarization is really low as well. Figure 10 shows the measured axial ratio and cross-polarization discrimination in the steering direction for each direction from  $-45^\circ$  to  $+45^\circ$ . These results allows to validate the different aspects of design and driving of this first prototype.

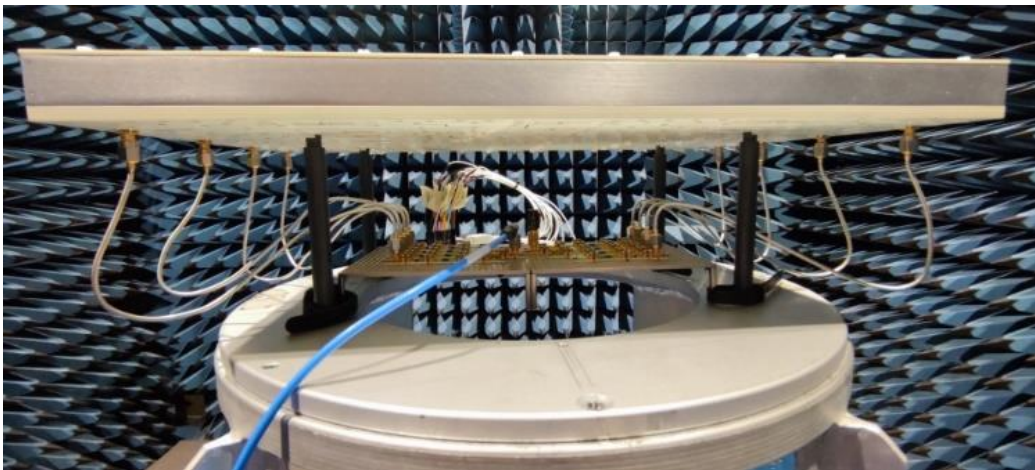


**Figure 7 4x4 panel with the X-Microwave board inside the anechoic chamber.**

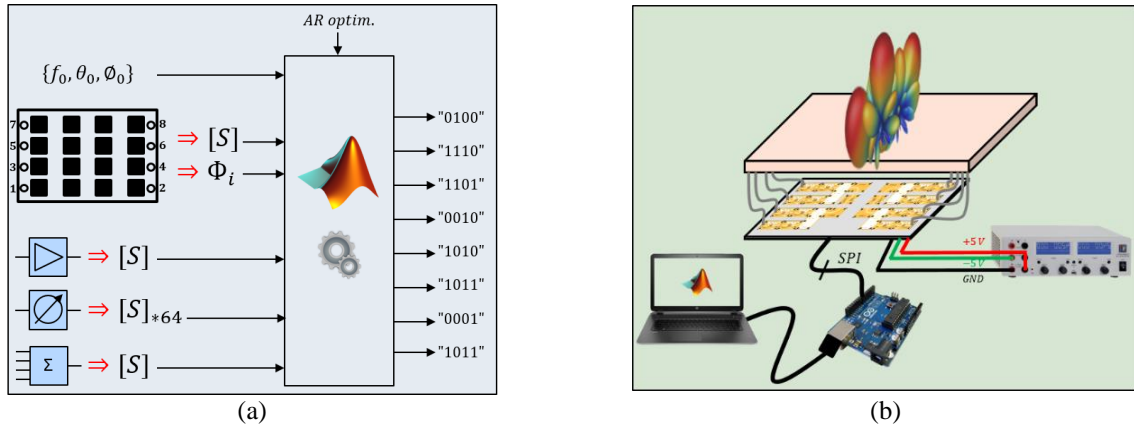


Figure 8 Characterization and driving bench: computing part (a) and driving part (b).

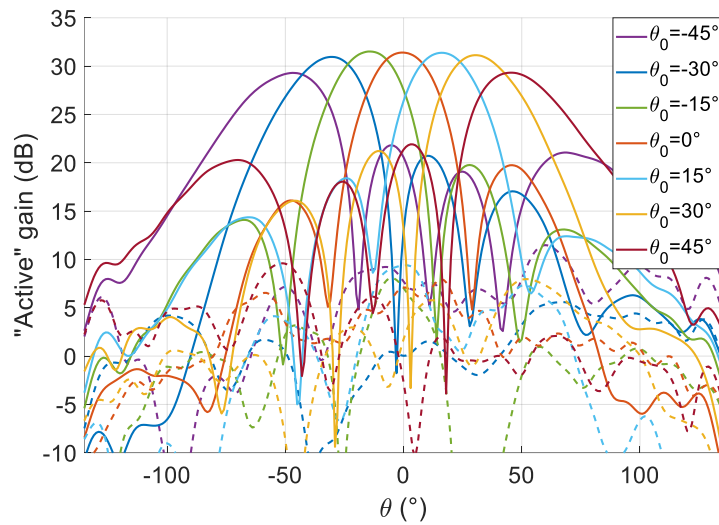


Figure 9 Measured radiation patterns of the 4x4 panel in RHCP at 2.25 GHz..

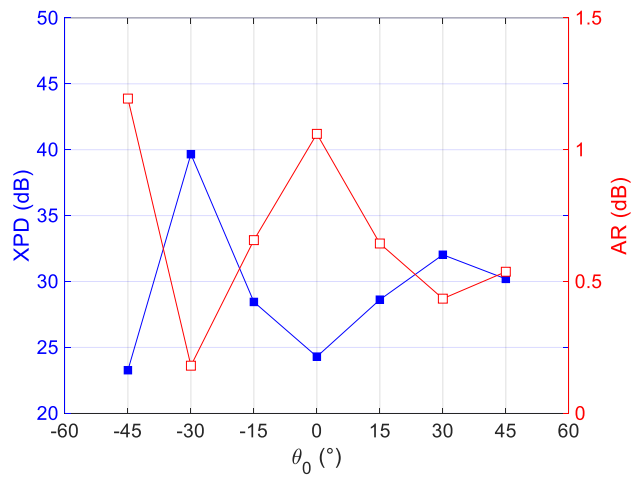


Figure 10 Measured XPD and AR in RHCP at 2.25 GHz function of steering direction.

## CONCLUSIONS

The principle and architecture of a hybrid mechanical/electrical scanning antenna were described. Then, the design of a dual polarization radiating unit-cell of which the performance was optimized over the required bandwidth and angular spectrum was presented. Finally, experimental results allowed to validate the operation of the 4x4 panel and to tackle future works with confidence.

## ACKNOWLEDGMENTS

The authors wish to thank the French Space Agency (CNES) for supporting this work through contract R&T R-S20/TC-0006-048-92.

## REFERENCES

- [1] <https://www.safran-group.com/fr/produits-services/antennes-fixes-mobiles-poursuite-telemesure-comtrack-sparte-300-sparte-500-sparte-700-tri-band-feed>
- [2] S. M. Sherman, D. K. Barton, *Monopulse Principles and Techniques*, 2nd ed. Artech House, 2011
- [3] <https://www.xmicrowave.com/>
- [4] F. Croq and D. M. Pozar, "Millimeter-wave design of wide-band aperture-coupled stacked microstrip antennas," in *IEEE Trans. Antennas Propag.*, vol. 39, no. 12, pp. 1770-1776, Dec. 1991
- [5] A. Hulzinga, J. Verpoorte, N. Venkatarayalu, and A. Thain, "Development of a broadband stacked patch antenna element for Ku-band phased array antenna" European Space Research and Technology Centre (ESTEC), 10 2012, pp. 3-5.
- [6] T. Chaloun, V. Ziegler, and W. Menzel, "Design of a dual-polarized stacked patch antenna for wide-angle scanning reflectarrays," *IEEE Transactions on Antennas and Propagation*, vol. 64, no. 8, pp. 3380-3390, Aug 2016.
- [7] D. M. Pozar and S. D. Targonski, "Improved coupling for aperture coupled microstrip antennas," *Electronics Letters*, vol. 27, no. 13, pp. 1129-1131, June 1991.
- [8] R. Lamey, M. Thevenot, C. Menudier, E. Arnaud, O. Maas and F. Fezai, "Interleaved Parasitic Arrays Antenna (IPAA) for Active VSWR Mitigation in Large Phased Array Antennas With Wide-Angle Scanning Capacities," in *IEEE Access*, vol. 9, pp. 121015-121030, 2021.
- [9] A. K. Bhattacharyya, *Phased Array Antennas: Floquet analysis, synthesis, BFNs, and active array systems*. John Wiley & Sons, 2006
- [10] R. J. Mailloux, *Phased array antenna handbook*, 2nd ed. Artech House, 2003 Consultive Committee for Space Data Systems (CCSDS), "Low density parity check codes for use in near-Earth and deep space applications (131.1-O-2 Orange Book)," Sep. 2007.